**Conference paper**

Tugce Bekat and Mualla Oner*

# Effects of ZnO crystals synthesized in presence of CMI biopolymer on PHBV properties

DOI 10.1515/pac-2016-0811

**Abstract:** Rod-shaped ZnO crystals were synthesized by chemical precipitation method from aqueous solution. Carboxymethyl inulin (CMI) was used as an additive in ZnO synthesis reaction, and particles with differing sizes and structures were obtained. CMI hindered crystal growth in the length axis of the rods, while growth on the lateral axis was not suppressed. ZnO crystals synthesized with varying CMI concentrations were incorporated into PHBV (3-polyhydroxybutyrate-*co*-3-hydroxyvalerate) matrix and the effect of the particles on thermal and mechanical properties of the polymer were investigated. Considerably good particle dispersion was obtained in the polymer matrix by melt-extrusion method. ZnO particles did not seem to affect main crystal structure, melting temperature and crystallization temperature of PHBV, whereas they had a retarding effect on crystallization. The addition of ZnO particles into PHBV increased elongation at break and toughness values, along with the decrease in the degree of crystallinity. Tensile strength was also increased without a significant change on the stiffness. Thermal degradation temperatures were observed to slightly decrease with ZnO addition compared to neat PHB; however, degradation peak temperature was still considerably above the melting temperature of the polymer.

**Keywords:** 3-polyhydroxybutyrate-co-3-hydroxyvalerate; biocomposites; carboxymethyl inulin; crystal growth; mechanical properties; PHBV; POC-16; thermal properties; zinc oxide.

## Introduction

ZnO particles are biocompatible materials with a broad range of applications due to their versatile properties [1, 2]. Incorporation of ZnO particles into polymer matrices for the purpose of polymer properties enhancement is one of the prominent application areas [3–8]. Properties of ZnO particles in end use applications strongly depend on particle shape, size and morphology; and various synthesis methods of ZnO particles offer a wide range of structures [9, 10]. Synthesis of uniform and monodisperse particles with controlled size and shape is essential in order to tailor properties of particles for specific applications. Among various synthesis methods of ZnO particles, wet chemical synthesis from aqueous solutions provides the advantages of simplicity, low operating temperatures, inexpensive, and high product yields [11, 12].

Water-soluble polymers are known to be effective tools in crystal synthesis for altering crystallization habit and modifying inorganic particle structures [12–15]. Carboxymethyl inulin (CMI) is a biodegradable,

**Article note:** A collection of invited papers based on presentations at the 16th International Conference on Polymers and Organic Chemistry (POC-16), Hersonissos (near Heraklion), Crete, Greece, 13–16 June 2016.

***Corresponding author: Mualla Oner,** Department of Chemical Engineering, Yildiz Technical University, Davutpasa Campus, Istanbul 34210, Turkey, Tel: +902123834740, Fax: +902123834725, E-mail: muallaoner@gmail.com
**Tugce Bekat:** Department of Chemical Engineering, Yildiz Technical University, Davutpasa Campus, Istanbul 34210, Turkey

eco-toxic, and sustainable water-soluble polymer; and has been used for crystal growth inhibition in the synthesis of several particles [16–19]. In a previous study of authors [12], CMI was reported to act as a crystal growth inhibitor for ZnO synthesis by the wet chemical method, altering the size and morphology of the particles. Crystallization reaction conditions strongly affected the final structure of the particles, as well. In this study, ZnO particles of different dimensions were synthesized using the same method with different reaction parameters. CMI was added to the crystallization reaction in varying concentrations, and its effect on crystal growth was evaluated. ZnO particles obtained in varying sizes were then incorporated into PHBV, a bio-based and biodegradable polymer. PHBV lacks some physical and thermal properties that limit its industrial usages, such as brittleness and low thermal stability. Possible enhancements in thermal and mechanical properties of PHBV with the addition of ZnO particles were investigated and the effects of particles synthesized with varying CMI concentrations were compared.

# Experimental

## Synthesis and characterization of ZnO crystals

ZnO crystals were synthesized by chemical precipitation method [12] from aqueous solution of zinc nitrate hexahydrate ($Zn(NO_3)_2 \cdot 6H_2O$, Fluka Analytical, 99 %) and hexamethylenetetramine [$(CH_2)_6N_4$, HMT, Merck, 99 %]. CMI (Dequest, PB11625) was added into the solution in varying concentrations. Crystallization reaction was carried out in a triple-neck jacketed vessel with 2 L capacity, connected to a thermostatic oil bath at 95 °C. Inlet concentrations of zinc nitrate hexahydrate and HMT were 0.06 M and the concentrations of CMI added were 0, 50, and 450 ppm. Reaction time was 90 min and the particles of CMI added were 0, 50, and 450 ppm. Reaction time was 90 min and the particles were separated from the suspension by filtration at the end of the reaction, followed by drying.

Synthesized ZnO particles were subjected to ultrasonic dispersion due to particle agglomeration using an ultrasonic horn (Sonics, Vibracell) of 13-mm diameter at 20 kHz frequency and 40% amplitude. Ultrasonication time was 60 min and was carried out under nitrogen cooling.

Scanning electron microscopy (SEM) images of the particles were taken using Zeiss EVO-LS at an accelerating voltage of 10.0 kV. Samples were coated by Au–Pd prior to the examination.

Fourier transform infrared spectroscopy (FTIR) analysis was performed using Bruker Optics Alpha-P, in the 400–4000 $cm^{-1}$ region and at a resolution of 4 $cm^{-1}$. Spectra were obtained by collecting the average of at least 20 scans.

## Incorporation of ZnO crystals into PHBV matrix

ZnO crystals synthesized with different concentrations of CMI (0, 50, and 450 ppm) were incorporated into PHBV (AdMajoris Company, Maj'Eco FN000HA) matrix by melt-extrusion method. A twin-screw extruder (Rondol, 10 mm Microlab, $L/D = 20$) was used with a temperature profile of 90-135-160-160-150 °C from feed to die and a screw speed of 80 rpm. PHBV/ZnO composite pellets obtained after extrusion were compression molded into sheets of 0.8 mm thickness using a mechanical press operated at 165 °C temperature and 30, 70, and 90 bar consecutive pressures.

## Characterization of PHBV/ZnO composites

SEM images of PHBV/ZnO composites were taken by Philips XL30 ESEM-FEG at an accelerating voltage of 5.0 kV. Samples were coated with Au prior to the examination.

Melting and crystallization behavior of PHBV samples was analyzed by differential scanning calorimetry (DSC). Samples of 10 mg mass were analyzed using Perkin Elmer, Pyris 1 under a nitrogen atmosphere. Samples were heated from 0 °C to 190 °C at a heating rate of 10 °C/min, and kept at this temperature for 2 min to erase thermal history. Then the samples were cooled to 0 °C at a cooling rate of 10 °C/min. Melting and crystallization temperatures and enthalpies were calculated from the heating and cooling curves. The degree of crystallinity ($X_c$) was calculated from the equation; $X_c$, $\% = \Delta H_m/\Delta H^0 * 100/w$, where $\Delta H^0$ is the melting enthalpy of 100% crystalline PHBV (146 J/g [20]) and $w$ is the weight fraction of PHBV.

Thermogravimetry analysis (TGA) was performed to evaluate the thermal stability of PHBV samples. Perkin Elmer, Pyris Diamond thermal analysis instrument was used. Samples of 10 mg mass were heated from room temperature to 550 °C with a heating rate of 10° min and under nitrogen flow. Peak degradation temperature ($T_{max}$) values were determined from the derivative TG curves, and initial degradation temperature ($T_i$) was calculated as the temperature corresponding to 2 % of weight loss.

Mechanical properties of the samples were analyzed by uniaxial tensile testing according to ASTM D882-12 standard. Instron 5982 universal testing machine was used with an initial load of 1 N and the crosshead speed was 5 mm/min.

# Results and discussion

## Formation of ZnO crystals and the effect of CMI

In absence of CMI, formation reaction of ZnO precipitate from the aqueous solution of zinc nitrate hexahydrate and HMT took place according to the following reaction steps [12]:

$$(CH_2)_6N_4 + 6H_2O \rightarrow 6HCHO + 4NH_3 \quad (1)$$

$$NH_3 + H_2O \rightarrow NH_4^+ + OH^- \quad (2)$$

$$Zn^{+2} + 2OH^- \rightarrow ZnO + H_2O \quad (3)$$

Rod-shaped, hexagonal prismatic ZnO crystals were obtained at the end of the crystallization reaction (Fig. 1a). When CMI was added to the reaction, the growth of crystals in the axis of length was limited, whereas crystal growth in the lateral face was not suppressed. The addition of CMI resulted in the production of shorter and thicker crystals, and this effect was more pronounced as the concentration of CMI was increased (Fig. 1b and

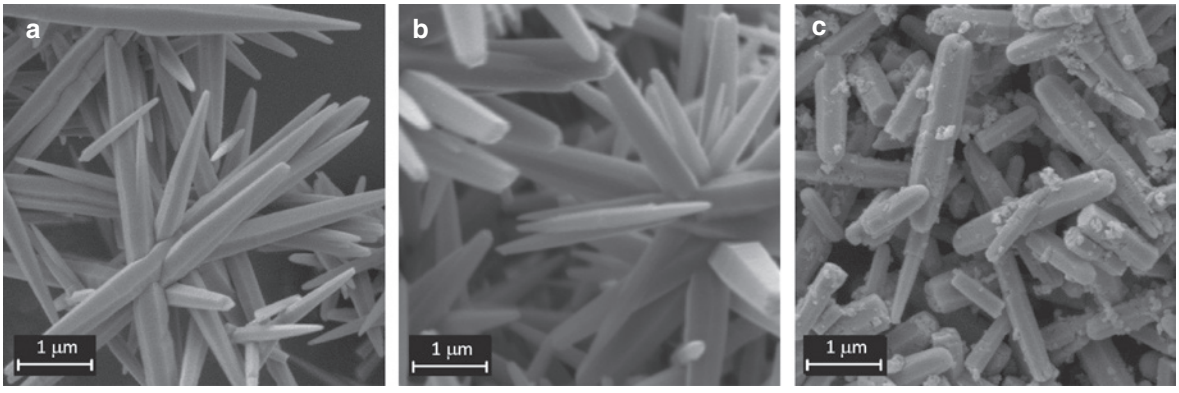


**Fig. 1:** SEM images of ZnO particles synthesized (a) without CMI addition, and (b) with 50 ppm and (c) with 450 ppm CMI addition.

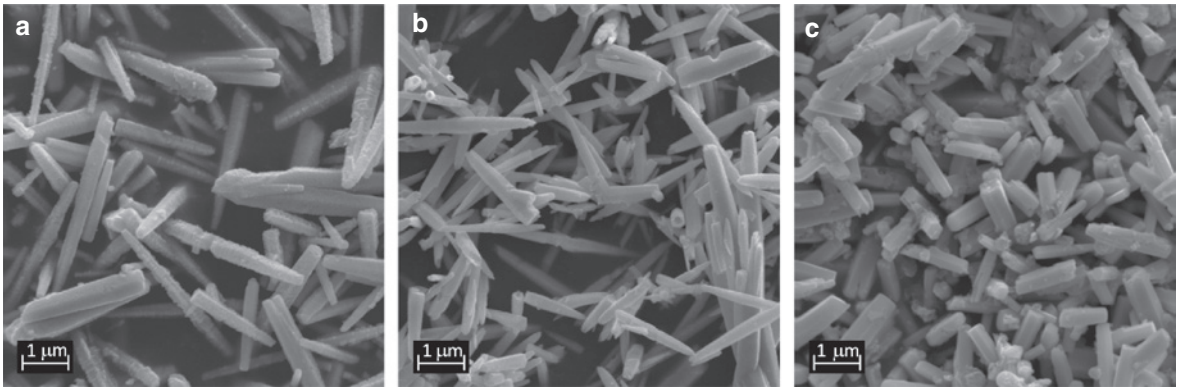


**Fig. 2:** SEM images of ZnO particles after ultrasound application (a) without CMI addition, and (b) with 50 ppm and (c) with 450 ppm CMI addition.

**Table 1:** Size distribution of ZnO particles after ultrasonic dispersion.

| Sample code | CMI concentration (ppm) | $L_{mean}$ (nm) | $D_{mean}$ (nm) | $L_{mean}/D_{mean}$ |
|---|---|---|---|---|
| ZnO | 0 | 3590.1 ± 1882.4 | 393.6 ± 124.4 | 9.1 |
| ZnO(50) | 50 | 3289.7 ± 1617.0 | 461.7 ± 200.7 | 7.1 |
| ZnO(450) | 450 | 2160.8 ± 765.8 | 510.2 ± 157.3 | 4.2 |

c). Formation of ZnO rod arrays connecting to each other at the center was observed for the particles synthesized in absence of CMI and with 50 ppm of CMI addition. This behavior was previously explained by a self-aggregation process occurring at high reaction temperatures [12]. When CMI concentration was increased to 450 ppm, the aggregated asterisk-like structures were no longer observed, and singular rod particles were obtained. It is well known that high surface energy of small particles lead to particle agglomeration and this effect might have been hindered for the higher concentration of CMI due to the increased diameter of particles.

Particle agglomeration is an undesirable phenomenon in the fabrication of polymer composites since it affects polymer properties negatively. Ultrasonic dispersion was applied to the particles prior to inclusion into the polymer matrix since severe agglomeration was observed for the particles synthesized with no and 50 ppm CMI addition. Particles synthesized in presence of 450 ppm CMI were also subjected to ultrasound for comparison purpose. SEM images of particles after 60 min of ultrasound application are given in Fig. 2. Ultrasound application was effective in breakage of aggregated array structures and singular, separated rod particles were obtained. For the particles synthesized with 450 ppm CMI addition, small crystal imperfections observed on the surface of the crystals prior to ultrasonication were ruptured and segregated by ultrasonic dispersion.

Mean length and diameter values of the particles were calculated after deagglomeration by ultrasound application. Statistical analysis was performed on SEM images taking at least 100 particles into consideration, and the mean values of crystal length, diameter and aspect ratio ($L/D$) are given in Table 1. $D$ is defined as the highest distance between opposite corners across the hexagonal face, measured at the thickest part of the crystals; and $L$ is the extension normal to the hexagonal face. Standard deviation values calculated for the mean length and diameter were relatively high due to the breakage of ZnO rods by ultrasound application, although more monodisperse particles were synthesized by crystallization reaction before the application of ultrasound. Increasing CMI concentration clearly produced shorter and thicker crystals.

FTIR analysis was applied to evaluate surface chemistry of the particles. The peak observed around 400 $cm^{-1}$ is the characteristic peak related to Zn-O stretching (Fig. 3). The peaks observed at 1325–1590 $cm^{-1}$ range were attributed to the carbonyl group in CMI molecule [21]. These peaks vaguely appeared on the spectrum of ZnO(50) sample, whereas were clearly observed on the spectrum of ZnO(450). The appearance of these peaks suggested CMI molecules were either chemically bonded or physically adsorbed on ZnO crystals.

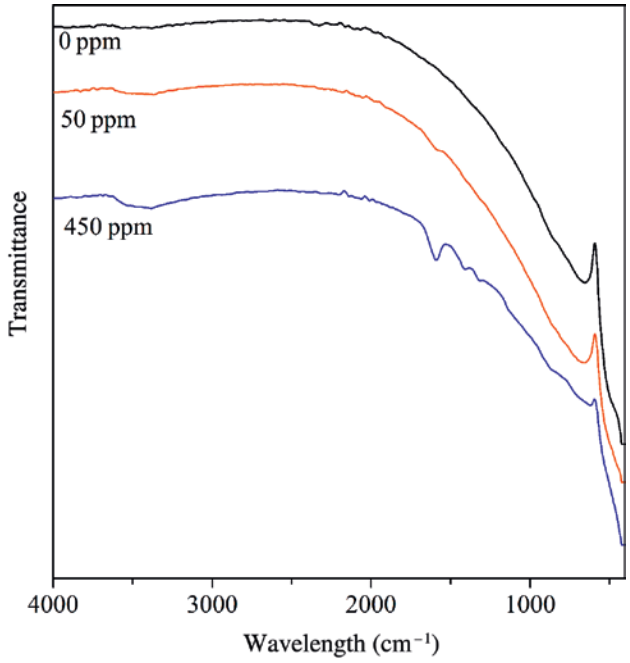


**Fig. 3:** FTIR spectra of ZnO particles synthesized with varying CMI concentration.

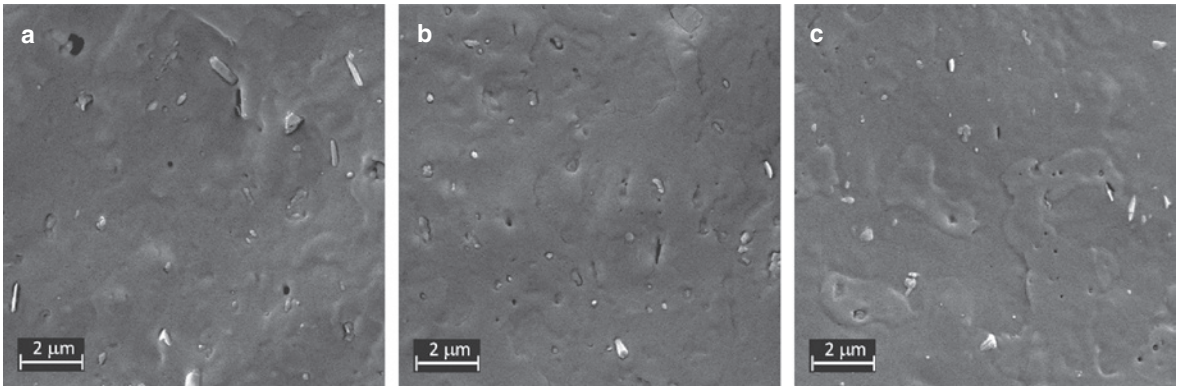


**Fig. 4:** SEM images of the composites (a) PHBV/ZnO, (b) PHBV/ZnO(50), and (c) PHBV/ZnO(450).

## Fabrication and characterization of PHBV/ZnO composites

Ultrasound dispersed ZnO, ZnO(50), and ZnO(450) crystals were incorporated into PHBV matrix by melt-extrusion. Particle content of the PHBV composites was selected as 1% (w/w) since homogeneous particle dispersion within the matrix is easier for lower particle loadings. SEM images of the composites fabricated are given in Fig. 4, indicating considerably good particle dispersion for all samples.

PHBV samples displayed bimodal melting behavior in DSC heating scan (Fig. 5a). Two-peak melting curves are common for PHBV samples [22] and are explained by a melting-crystallization-remelting behavior [23]. The appearance of the first melting peak ($T_{m1}$) was around 174 °C and the second melting peak ($T_{m2}$) was around 181 °C for all samples (Table 2), suggesting main crystal structure and lamellar size was not affected by ZnO addition. However, total enthalpy of fusion ($\Delta H_m$) and thus $X_c$ were decreased in composite samples compared to neat PHBV. ZnO particles had a retarding effect on nucleation, decreasing the degree of crystallinity. The intensity of second melting peaks was increased compared to neat PHBV, probably due to the increased mobility of polymer chains and recrystallization of more crystals into more stable crystals. This effect was more

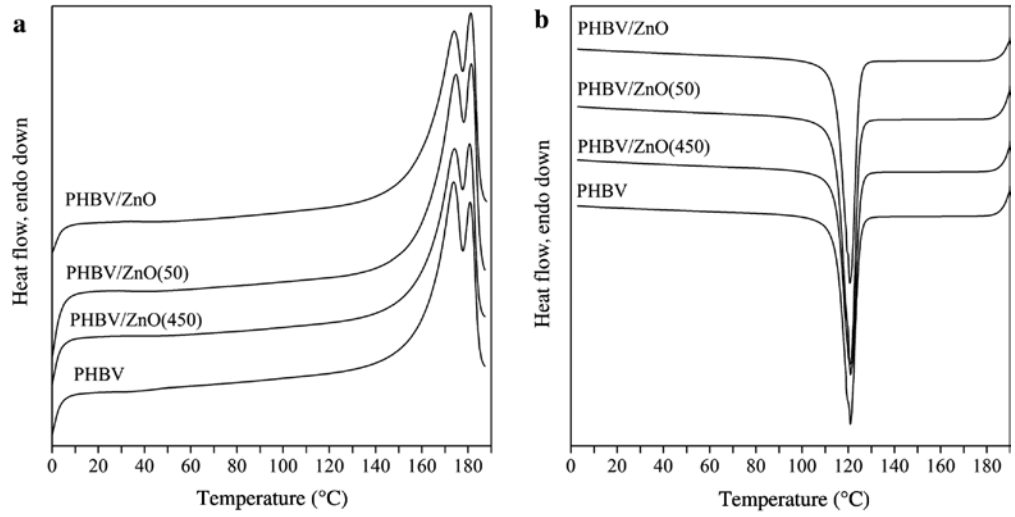


**Fig. 5:** DSC thermograms of PHBV and its composites: (a) heating and (b) cooling scans.

**Table 2:** Thermal properties of PHBV and its composites obtained by DSC and TG analyses.

| Sample code | Heating scan | | | $X_c$ (%) | Cooling scan | | $T_i$ °C | $T_{max}$ °C |
|---|---|---|---|---|---|---|---|---|
| | $T_{m1}$ °C | $T_{m2}$ °C | $\Delta H_m$ (J/g) | | $T_c$ °C | $\Delta H_c$ (J/g) | | |
| PHBV | 173.7 | 181.0 | 111.3 | 76.3 | 120.9 | −107.2 | 263.9 | 284.5 |
| PHBV/ZnO | 174.2 | 181.1 | 101.0 | 69.9 | 120.6 | −93.3 | 258.6 | 277.1 |
| PHBV/ZnO(50) | 174.4 | 181.3 | 102.3 | 70.8 | 120.7 | −104.4 | 256.1 | 275.2 |
| PHBV/ZnO(450) | 173.7 | 180.6 | 101.3 | 70.1 | 121.0 | −94.2 | 257.8 | 277.1 |

pronounced for the PHBV/ZnO and PHBV/ZnO(50) composites. PHBV and its composites exhibited similar cooling scan curves (Fig. 5b), with a crystallization temperature ($T_c$) around 121 °C. The decrease in crystallization enthalpy ($\Delta H_c$) with ZnO addition also suggested a decrease in the degree of crystallinity of PHBV.

ZnO particles were previously reported to accelerate crystallization of PHB (polyhydroxybutyrate) [24] and PHBV [25] due to heterogeneous nucleation effect. On the other hand, another study [26] reported the retarding effect of ZnO particles on crystallization of electrospun PHBV nanofibers, decreasing crystallinity while showing no effect on the value of $T_m$. This behavior was explained by the formation of hydrogen bonds between the ZnO particles and PHBV, disturbing the mobility of PHBV chains and decreasing crystallinity.

TGA analysis revealed that addition of ZnO particles slightly decreased the degradation temperatures $T_i$ and $T_{max}$ compared to neat PHBV sample (Table 2). Fortunately, the $T_{max}$ values obtained were considerably above the $T_m$ values, only slightly narrowing the processing window of the polymer. considerably above the $T_m$ values, only slightly narrowing the processing window of the polymer. Decrease in thermal stability was previously reported for incorporation of cellulose nanowhiskers [27] and graphene [28] into PHBV matrix. The increase of thermal conductivity of the matrix due to the addition of particles was reported to have a negative effect on thermal degradation.

Tensile strength, Young's modulus, and elongation at break values were calculated for PHBV and its composites from the stress-strain curves obtained from tensile testing (Figure 6). ZnO particles might have contributed to effective stress transfer across the polymer matrix, since tensile strength was observed to increase with ZnO addition into PHBV. Young's modulus values were not affected significantly. Toughness values were calculated as the area underneath the stress-strain curves. The addition of ZnO particles into PHBV matrix significantly increased elongation at break and toughness of the polymer. These results were in correspondence with DSC findings, since lower crystallinity is known to result in higher ductility. The increase in ductility is important since one of the major drawbacks of PHBV is its brittle nature. Increase

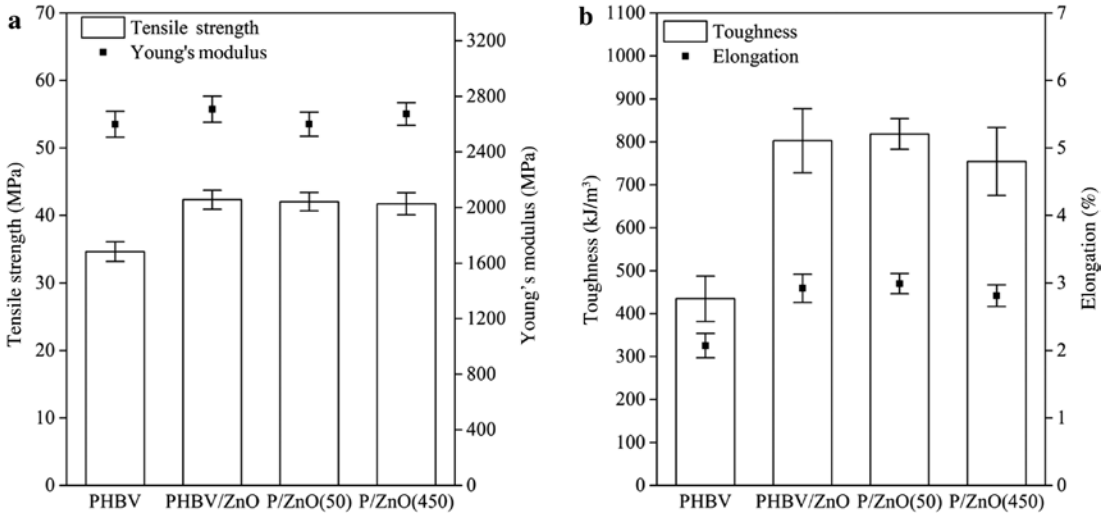


**Fig. 6:** Tensile properties of PHBV samples: (a) tensile strength and modulus, and (b) toughness and elongation at break.

in elongation and toughness were higher for PHBV/ZnO and PHBV/ZnO(50) samples, compared to PHBV/ZnO(450) sample. Aspect ratio ($L/D$) of particles is known to be an effective parameter in ductility, as well as crystallinity, affecting the shear stress at the filler-matrix interface. This could be the reason for higher toughness values obtained for composites fabricated with ZnO particles with higher $L/D$ values.

## Conclusion

ZnO crystals of different dimensions and aspect ratios were synthesized in presence of CMI as a crystal growth inhibitor. CMI inhibited the growth on the length axis of ZnO rods, producing shorter and thicker crystals. ZnO crystals synthesized in absence of CMI or with low concentrations of CMI added, tended to form self-aggregated asterisk-like structures, whereas this behavior was not observed when CMI concentration was increased. Ultrasonic dispersion was an effective method in breakage of self-aggregated structures, producing separated, singular ZnO rods.

Incorporation of ZnO particles into PHBV matrix decreased crystallinity of the polymer and helped enhancement of ductility. Main crystal structure, melting and crystallization temperatures of PHBV were not affected by ZnO addition. Thermal degradation temperatures were slightly decreased. The concentration of CMI in ZnO synthesis did not show any significant effect on the properties of PHBV/ZnO composites.

**Acknowledgement:** The authors would like to thank Yildiz Technical University Scientific Research Projects Coordinator for financial support on Project no. 2015-07-01-DOP03.

## References

[1] P. Kumar, Y. K. Walia. *Asian J. Of Adv. Basic Sci.* **2**, 39 (2014).
[2] C. Y. Chen, M. W. Chen, J. J. Ke, C. A. Lin, J. R. D. Retamal, J. H. He. *Pure Appl. Chem.* **82**, 2055 (2010).
[3] M. Murariu, A. Doumbia, L. Bonnaud, A. L. Dechief, Y. Paint, M. Ferreira, C. Campagne, E. Devaux, P. Dubois. *Biomacromolecules* **12**, 1762 (2011).
[4] M. Derradji, N. Ramdani, L. Gong, J. Wang, X. Xu, Z. Lin, A. Henniche, W. Liu. *Polym. Advan. Technol.* **27**, 882 (2016).
[5] P. Atayev, T. Bekat, M. Oner. *Sigma J. Eng. Nat. Sci.* **33**, 16 (2015).
[6] M. Sato, A. Kawata, S. Morito, Y. Sato, I. Yamaguchi. *Eur. Polym. J.* **44**, 3430 (2008).
[7] N. Lu, X. Lu, X. Jin, C. Lu. *Polym. Int.* **56**, 138 (2007).

[8] E. G. Ahangar, M. H. A. Fard, N. Shahatahmassebi, M. Khojastehpour, P. Maddahi. *J. Food Process. Pres*. **39**, 1442 (2015).
[9] A. K. Radzimska, T. Jesionowski. *Materials* **7**, 2833 (2014).
[10] Z. L. Wang. *Mater. Today* **7**, 26 (2004).
[11] S. S. Guzman, B. R. Jayan, E. Rosa, A. T. Castro, V. G. Gonzalez, M. J. Yacaman. *Mater. Chem. Phys*. **115**, 172 (2009).
[12] B. Akin, M. Oner. *Res. Chem. Intermed*. **38**, 1511 (2012).
[13] Y. F. Gao, H. Y. Miao, H. J. Luo, M. Nagai. *Cryst. Growth Des*. **8**, 2187 (2008).
[14] Q. Huang, T. Cun, W. zuo, J. Liu. *Appl. Surf. Sci*. **332**, 581 (2015).
[15] B. Panigraphy, M. Aslam, D. S. Misra, D. Bahadur. *CrystEngComm*. **11**, 1920 (2009).
[16] D. L. Verraest, J. A. Peters, H. Bekkum, G. M. Rosmalen. *J. Am. Oil Chem. Soc*. **73**, 55 (1996).
[17] L. Boels, G. J. Witkamp. *Cryst. Growth Des*. **11**, 4155 (2011).
[18] B. Akin, M. Oner, Y. Bayram, K. D. Demadis. *Cryst. Growth Des*. **8**, 1997 (2008).
[19] O. Dogan, M. Oner, O. Cinel. *J. Ceram. Soc. Jpn*. **118**, 579 (2010).
[20] P. J. Barham, A. Keller, E. L. Otun. *J. Mater. Sci*. **19**, 2781 (1984).
[21] M. Oner, U. Uysal. *Mater. Sci. Eng. C* **33**, 482 (2013).
[22] E. Bugnicourt, P. Cinelli, A. Lazzeri, V. Alvarez. *Express Polym. Lett*. **8**, 791 (2014).
[23] L. M. W. K. Gunaratne, R. A. Shanks. *Eur. Polym. J*. **41**, 2980 (2005).
[24] A. M. D. Pascual, A. L. D. Vicente. *Int. J. Mol. Sci*. **15**, 10950 (2014).
[25] A. M. D. Pascual, A. L. D. Vicente. *ACS Appl. Mater. Interfaces*. **6**, 9822 (2014).
[26] W. Yu, C. H. Lan, S. J. Wang, P. F. Fang, Y. M. Sun. *Polymer* **51**, 2403 (2010).
[27] E. Ten, J. Turtle, D. Bahr, L. Jiang, M. Wolcott. *Polymer* **51**, 2652 (2010).
[28] J. A. Martin, G. Gorrasi, A. L. Rubio, M. J. Fabra, L. C. Mas, M. A. L. Manchado, J. M. Lagaron. *J. Appl. Polym. Sci*. **132**, 42101 (2015).